"On-Body Channel Measurement using Wireless Sensors", Max O. Munoz, Robert Foster and Yang Hao, IEEE Transactions on Antennas and Propagation, vol. 60, no. 7, pp. 3397-3406, 2012.

This post-acceptance version of the paper is essentially complete, but may differ from the official copy of record, which can be found at the following web location (subscription required to access full paper): http://dx.doi.org/10.1109/TAP.2012.2196933

On-Body Channel Measurement using Wireless Sensors

Max O. Munoz, Robert Foster, *Member, IEEE*, Yang Hao, *Senior Member, IEEE*

***Abstract*—The on-body channel was characterised at various points on the human torso in an anechoic chamber using a pair of wireless sensor modules. The performance of wireless IEEE 802.15.4 sensor nodes operating in the 2.45 GHz ISM frequency band (2.40-2.4835 GHz) is presented over each of the 16 different channels. It is shown that the response at individual carrier frequencies is dependent not only on the initial antenna response, as determined by the on-body measurement in isolation, but also on the overall system performance. Measurement results are also compared with those from the conventional technique using a Vector Network Analyzer.**

***Index Terms*—Wearable antenna, on-body wireless sensors, channel performance, electromagnetic wave propagation, medical applications, body-centric communication.**

I. Introduction

THERE has been rapid growth in the number of wireless devices operating in close proximity to the human body in recent years. The design of small antennas that can provide high efficiency, immunity to frequency detuning, immunity to pattern fragmentation and operation at different frequencies whilst close to, on or even within the body, are current topics of active research [1, 2]. Improving our understanding of the on-body propagation channel is central to being able to properly design antennas for the environment.

Thus far, it has proved difficult to separate the observed on-body propagation channel and antenna characteristics, unlike in free-space environments. It has been recognised for some time that operation on or near the human body is far from a free-space environment [1]; hence, to understand on-body behaviour, on-body measurements must be taken. The standard methods for characterising propagation and antenna performance typically utilise a vector network analyzer (VNA), or an RF source and spectrum analyzer (SA). To date, most on-body measurements have continued to use the VNA or SA approach (e.g., [3], [4]).

However, the coaxial cable connecting antenna and VNA can often introduce error, due to unwanted radiation from currents flowing on the outer surface of the cable, as well as errors from cable movements. Alternative techniques have been explored to mitigate this 'cable effect', including the use of fibre-optic systems (see, for example, [5]; also [6-8]). Fibre-optic cables are essentially immune to electromagnetic interference (EMI) and radio frequency interference (RFI), which have a major impact on traditional on-body measurements (VNA and coaxial cables). In [9], off-body measurements were performed in an anechoic chamber and indoor environment using a fibre-optic system on a motionless test subject. The effect on measured data by the method of measuring can still be significant, especially when a dynamic human body scenario is considered (e.g., jogging). The motion may bend the fibre-optic cable, introducing changes in the polarization planes, as well as fluctuations in temperature, leading to changes in the sensitivity of the fibre-mounted sensor [10]. In addition, the fibre optic system usually contains an electrically large optical modulator/demodulator which can cause scattering to on-body radio waves.

Furthermore, the antenna will behave differently when measured in isolation and when integrated with a system, as required in any application (a fact that has influenced mobile phone antenna design for some time; see, for example, [11-13]), due to additional surface currents induced on the system structure. This will, in turn, affect the propagation channel data, due to the difficulty in decoupling the two aspects. In this paper, a measurement technique is investigated that uses the commonly-available received signal strength (RSS) figure-of-merit to determine propagation characteristics for a number of wireless sensor modules, using two identical microstrip patch antennas to ensure the effect of the antenna is minimized. These measurements are compared to others made using the conventional VNA technique. The study described below evaluates the channel performance of each frequency carrier for IEEE 802.15.4 sensor nodes operating in the 2.45 GHz ISM band (2.40-2.4835 GHz). The effect of the carrier frequency and antenna radiation performance are also investigated from the system point of view. For this initial study, only a motionless (static) subject was considered; dynamic scenarios are reserved for future work.

The rest of the paper is organised as follows: Section II provides background on the motivation for this work, together with information on related work. Section III describes the measurement procedures used in this study and provides some initial measured data for the devices used. Section IV presents the body of the results for the propagation channel. Finally, a summary is provided in Section V.

II. Motivation and Related Work

A. On-Body Communications

The interconnection of different wireless sensors around the human body defines a Wireless Body Area Network (WBAN).

Manuscript received June 17, 2011; revised November 11, 2011.

The authors are with the School of Electronic Engineering and Computer Science, Queen Mary College, University of London, United Kingdom. Email: {max.munoz | robert.foster | yang.hao}@eecs.qmul.ac.uk.

Each pair of nodes has an independent radio communication link [1, 2]; each link exhibits different channel characteristics, due to the fact that unique areas of the body will have different features and properties. In addition, external perturbations, such as human mobility and operation in diverse environments, create a complex scenario for the radio communications of wearable sensors [3], [4].

A noticeable evolution of technique can be traced in the history of on-body propagation channel measurements, whereby the measuring devices become smaller and the complete system is worn on-body. Early research into on-body wireless communications channels used standard measurement techniques, based around a VNA. One of the earliest papers [14] used flexible coaxial cables to connect two patch antennas to the VNA. The variation in cable loss due to body movements was estimated (by replacing the wireless link with semi-rigid coaxial cable) to be 0.1 dB across the frequency band of interest. No reference was made to the cable effect; the radiation patterns of the two patch antennas used were only characterised off-body.

In order to understand properly the effect of human motion on the channels, measurements were soon made with a Rhode and Schwartz FSH6 spectrum analyser with tracking generator, controlled by a small laptop, both carried by the subject in a small backpack [15, 16]. Flexible coaxial cables were again used to connect the antennas to the measuring equipment, whilst noting the potential for error from the presence of the cables, due to scattering and the potential for surface currents on the outside of the cable. However, neither quantifying nor eliminating the error from the cables was deemed possible. It is noted that the measuring equipment is fairly bulky and prohibits the investigation of some human movement, due to its restrictive position and weight.

In [17-20], on-body propagation models were investigated for indoor and outdoor scenarios using body-worn sensors communicating at 868 MHz and 2.45 GHz. The use of such sensors removed the need for cables on-body; the size and weight is also significantly less than SAs and laptops. The transmitter was placed at waist level and used a 2.0 dBi gain dipole antenna; the receivers, placed at different points on the body, were either based on Crossbow Mica2Dot wireless sensors (for 868 MHz) [17, 18]; or they were based on Linear Technology LT5504 RF modules (for 2.45 GHz) [19, 20]. Their results show that on-body propagation characteristics are dependent on user state and environment; however, it is noted that the transmitter output power for the experiments at 2.45 GHz was +22 dBm, which is unrealistic for real-world applications.

Furthermore, the transmitter used was a NovaSource G6 synthesized RF signal source, in continuous-wave mode, with an additional Hittite HMC-455LP3 amplifier for the 2.45 GHz experiments, rather than using a solution based purely on packet-radio hardware. The NovaSource G6 is still a relatively bulky item, measuring 70 mm x 102 mm x 19 mm (width by length by height) and weighing 170 g, not including the power supply and cables, with an aluminium case. The effect of this unit on the transmit antenna radiation pattern has not been discussed, either in free-space or on-body.

Other studies have been conducted over the past decade and reported in the literature. Most use either a VNA or Vector Signal Analyzer (e.g., [21-28]), or a source combined with a spectrum analyser (e.g., [29, 30]). In [31], Texas Instruments wireless nodes (i.e., CC2510 evaluation modules) and an RF packet sniffer (i.e., TI smart RF04EB board) were used to characterize the interaction and the performance of the physical layer for on/off-body communication links. A few studies characterized on-body radio links using wireless sensor nodes ([32-36]), but have not compared the obtained results with other measurement techniques, meaning sources of error remain uncertain.

This study investigates the potential for improving measurement capabilities on-body, by using small sensor nodes for both transmitter and receiver. A more realistic transmit power of 0 dBm will be used and the measurements will be packet-based, rather than continuous-wave. The CC2420 [37], an IEEE 802.15.4-compliant radio transceiver from Texas Instruments, will be used, with the modulation occurring on-chip. Comparisons with conventional measurements using a VNA will be made. One advantage of this approach is that it also provides insight into real-world, rather than laboratory, scenarios.

B. The Human Body

The human anatomy is formed of a three-dimensional multi-layer structure filled by heterogeneous tissues. In [38], measured values for a wide range of frequencies (10 Hz to 20 GHz) has been intensively studied and characterised. Table I lists the electrical properties of some human tissues concealed in the thoracic section of the body at 2.45 GHz. More detailed lists can be found in [38-40].

This current work is focused on the thoracic section of the human body, as it represents the main area for a variety of healthcare applications, such as cardiac monitoring, respiratory sensors, pacemakers, gastric band controllers, bladder implants and others. The trunk includes a great variety of organs, with the associated variability in dielectric characteristics; it is also anticipated to be the most complex and irregular environment for electromagnetic modelling and, hence, for on-body radio links (Table I). It is noted that the characterisation of low power wireless channels depends upon many factors, some of which are not considered in this present study. These include the effect of individual subjects (for instance, short or tall, thin or fat), the surrounding environment, the type of activity and the application.

III. MEASUREMENT PROCEDURES

Measurements were performed on the thoracic area of a male test subject, measuring 170 cm in height and 78 kg in weight, standing motionless in an anechoic chamber. The transmitter antenna was placed on the right waist section of the body and the receiver antenna moved symmetrically along the trunk section. The antennas are located 3 cm away from

TABLE I
ELECTRIC PROPERTIES OF SPECIFIC HUMAN BODY TISSUES USED WITHIN THE VISIBLE MAN MODEL PROJECT AT 2.45 GHZ [38-40]

Tissue Name	Conductivity [S/m]	Relative Permittivity	Loss Tangent
Stomach	2.22810	62.126	0.26100
Fat	0.10540	5.2780	0.14532
Skin Dry	1.47340	37.984	0.28229
Muscle	1.75240	52.705	0.24197
Bone Marrow	0.09592	5.2947	0.13185

the body's surface. The area was divided into 30 different points (6 × 5 matrix points) using a 5 cm spacing, as shown in Fig. 1.

The current study uses a pair of microstrip patch antennas printed on top of a FR-4 substrate layer with thickness of 1.6 mm. Antenna dimensions and the measured and simulated reflection coefficients for the transmit and receive antennas are depicted in Figs. 2a and 2b. A summary of each antenna's radiation performance is presented in Table II.

Although each antenna has been manufactured using an identical design layout, it is understandable that the manufacturing and soldering procedure, such as the fitting of the connector, would introduce some systematic errors within the antenna's radiation performance.

A large ground area underneath the patch antenna usually mitigates the effects of the lossy human body tissues. In [41], a patch antenna of 0.49λ × 0.53λ was implemented, reporting a 10 MHz detuning when placed on-body. As a result, the initial antenna parameters (antenna alone in free-space) are influenced by the large volumetric section of the human body, introducing fluctuations in return loss (i.e., S_{11} depth) and frequency (detuning). These variations are related not only to on-body location, but also to movement, such as the breathing activities. Fig. 3 illustrates absolute fluctuations for the receiver antenna at each point alongside the trunk section. Table III summarises the mean deviation in S_{11} and frequency, for both transmit and receive antennas.

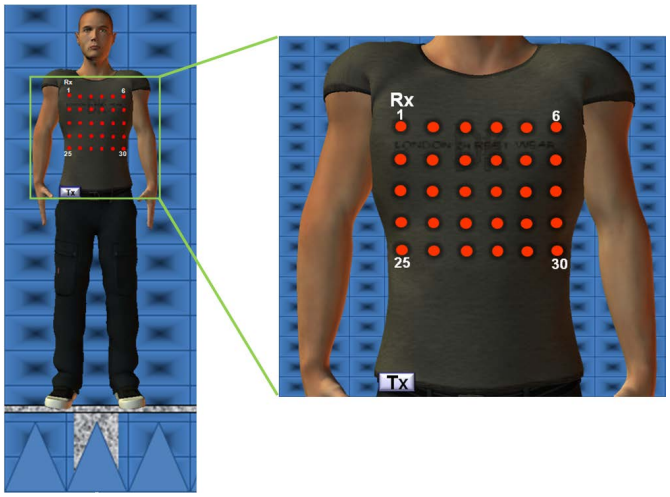

Fig. 1. Location of transmitter and receiver antennas used for each on-body measurement in an anechoic environment.

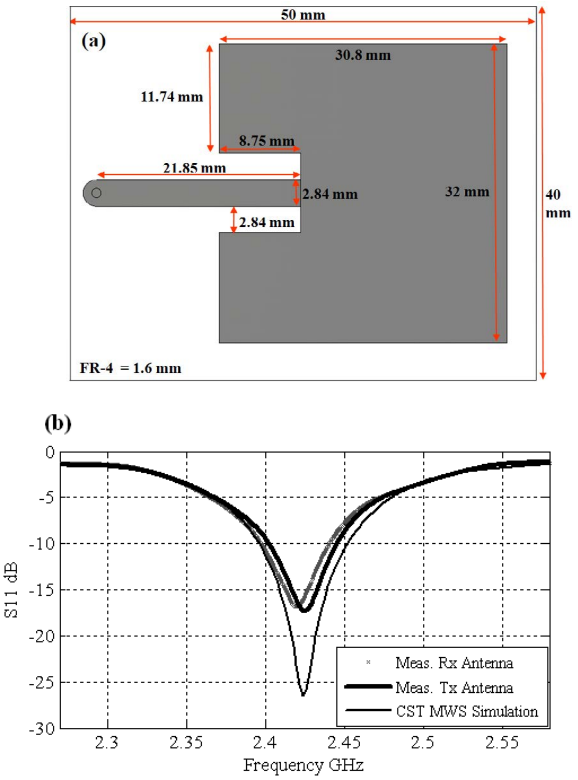

Fig. 2. Antenna used for on-body measurements: (a) design layout of a microstrip patch antenna; (b) simulated and measured S_{11} of patch antennas.

TABLE II
PARAMETRIC COMPARISON OF ANTENNA DESIGNS IN FREE SPACE SIMULATION AND MEASUREMENT

Antenna Location	Res. Freq. GHz	S11 dB	Gain dBi	BW %
Simulation	2.424	-26.52	3.8	2.39
Measured Rx. Antenna	2.419	-16.87	2.13	1.98
Measured Tx. Antenna	2.425	-17.32	2.15	1.96

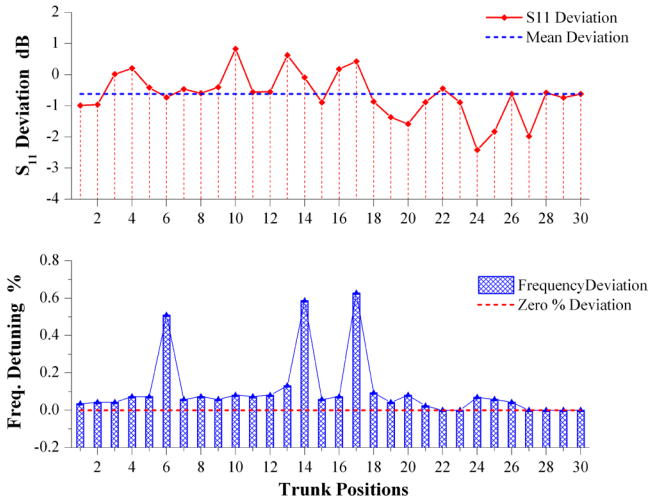

Fig. 3. On-body absolute frequency detuning and return loss deviation of the receiver antenna at each point on the trunk section, compared with free-space measurements. Both sets of measurements were taken using the VNA.

TABLE III
DEVIATION OF ANTENNA PARAMETERS WHEN PLACED ON-BODY

Antenna Location	Freq. Detuning %	S_{11} Mean Deviation dB	BW (*at -10 dB*) %
Rx. Antenna	0.001	-0.62	2.16 - 2.36
Tx. Antenna	0.0923	-2.69	2.06

The -10 dB impedance-matched bandwidth of the receiver antenna varies by 2.16% to 2.36%, clearly reflecting the human tissue variation alongside the trunk. On the other hand, the transmitter antenna, which preserves its location during the measurement procedure, has a maximum detuning of 2.24 MHz and a 2.06% bandwidth when on-body. It is evident that the fluctuations at this point are lower than the receiver locations. These results are important for understanding the collected measurement data, discussed below.

The wireless on-body radio channel measurements were divided into two groups, discussed below.

A. First Measurement Setup

The first measurement set was made with the aid of a Hewlett Packard 8720ES VNA, calibrated using standard techniques. These measurements were sub-divided in two parts:

- measurement of a stand-alone antenna (Fig. 4a), on-body, using coaxial cable (polystyrene foam was used for the mechanical support of the antenna);
- measurement of the antenna when in close proximity to the embedded system (i.e., the two are positioned close together, as if connected, but the measurement equipment was still connected with coaxial cable and no direct connection between antenna and embedded system existed; see Fig. 4b).

The frequency sweep was set from 2.4-2.5 GHz, with the maximum number of points (1601). The sweep time was 800 ms, with an output power of 0 dBm.

Five different measurements were taken over a period of five days, in order to obtain an averaged response for the test subject. In each measurement, two sets of data were recorded. The path loss at each point is calculated from the average of the 10 different samples sets of data.

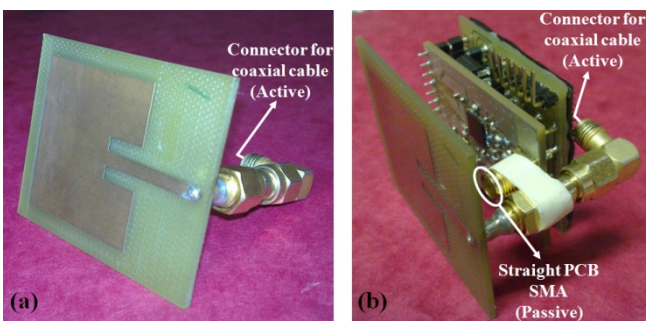

Fig. 4. Measurement of the microstrip patch antenna using a Vector Network Analyzer: (a) stand-alone antenna; (b) antenna with close proximity to the in-house wireless node. Note that the PCB SMA is not connected to SMA connector of the antenna (passive SMA).

These results are presented in Section IV, where they are combined with those obtained with the second measurement procedure (Section III-B) to aid comparison and understanding.

B. Second Measurement Setup

Two wireless sensor modules, designed and fabricated as part of this work, were used for the second measurement campaign. Each module used a Texas Instruments (TI) transceiver, the CC2420 [37]. The transceivers are programmed and controlled by an ultra-low-power microcontroller, the PIC18F2620 [42]. Each wireless module is powered by a 3.6V NIMH (Nickel Metal Hydride) battery, 25 mm x 15 mm in size, through external PCB terminals. Fig. 5a depicts the structure of each module, Fig. 5b shows the implemented modules, Fig. 5c illustrates the in-house wireless node showing the battery and Fig. 5d displays the TI evaluation board for the CC2420 with in-house control board and patch antenna. The TI evaluation board (see Fig. 5c) served two purposes in this work: first, to validate the performance of the in-house transceiver module (see Fig. 5b); second, to provide an alternative system for use in the wireless-sensor-based measurements described below. This allows a degree of verification of the measurement technique: by having two physically-different systems, differences between the two measurement techniques can be observed, whilst also considering the effects of the physical structure of the specific systems.

Each transceiver was programmed to operate with a maximum output power of 0 dBm; they each have a maximum sensitivity of -95 dBm, with an adjacent channel rejection of 45 dB. The frequency of operation for each module was updated, to measure each of the 16 channels. The MAC layer was programmed according to the guidelines of the IEEE 802.15.4 standard [43].

In order to decrease the error introduced by on-body position displacement (such as that introduced by conducting measurements over a period of five days), each wireless module was fitted using VELCRO tape to the thoracic area of the subject; the grid of locations was marked on the T-shirt worn by the test subject, enabling the position to be recaptured reasonably accurately in each subsequent measurement. In each location, the modules acquired an average of 8000 samples of the received signal (RSSI), recorded in the internal flash memory of the microcontroller. The obtained data was later extracted and analyzed; results are presented in Section IV.

The maximum output power at the antenna port of each wireless sensor was measured by a Rohde & Schwarz FSP 40 Spectrum Analyzer while transmitting continuously. The frequency was centred at 2.42 GHz, with a span of 300 MHz and a resolution bandwidth of 3 MHz. Fig. 6 shows the power spectrum of each module and Table IV lists the maximum output power measured using the *max-hold* function of the spectrum analyzer over a length of time (~10 minutes). This enable the best node for transmission to be determined (greatest output power).

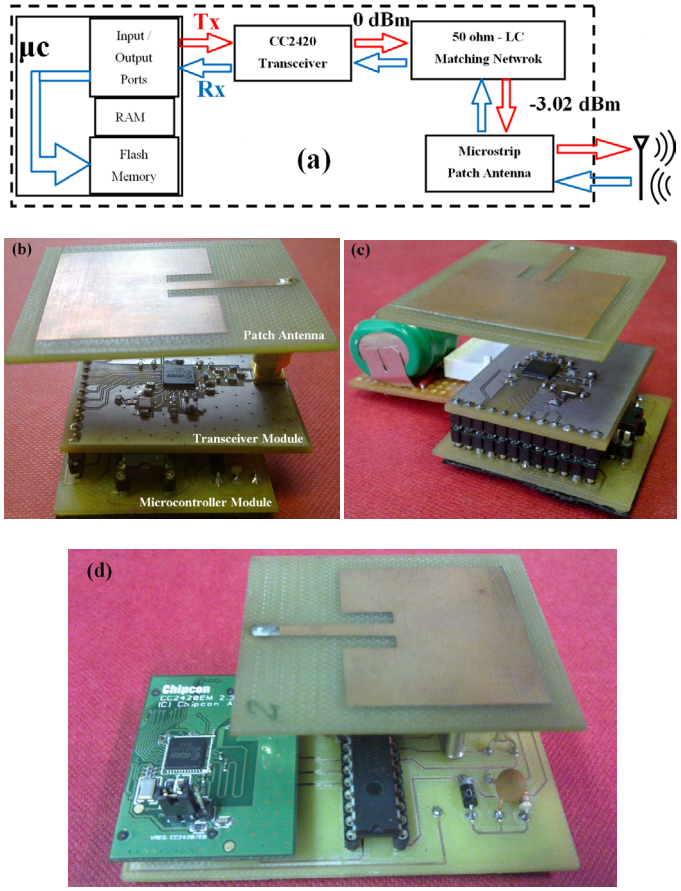

Fig. 5. Data Logging units used for on-body measurements: (a) internal wireless sensor structure; (b) implemented in-house wireless node using a microstrip patch antenna; (c) in-house wireless node showing the battery; (d) alternative wireless node using CC2420 evaluation modules from TI.

The use of λ/4 transmission lines for the 50 Ω impedance match on the Texas Instruments modules yields a better output power, -1.05 dBm; in contrast, the purposely-built modules utilize an L-C configuration outputting -3.02 dBm of initial power. Even though L-C networks make use of a smaller area on the PCB, they tend to introduce higher losses which are consequence of component size, type of dielectric and thermal resistance [44].

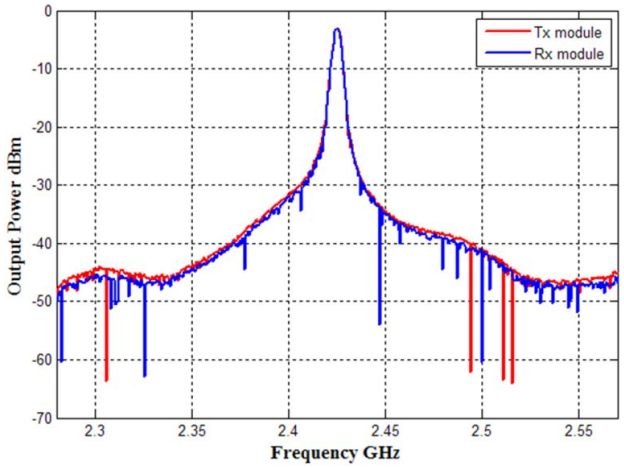

Fig. 6. Power Spectrum Response for the transmitter and receiver wireless sensor nodes, measured using the *max-hold* function of the spectrum analyzer.

TABLE IV
POWER SPECTRUM OF INDIVIDUAL WIRELESS SENSORS USED FOR ON-BODY MEASUREMENTS

Wireless Modules	Max. Output Power dBm	Frequency GHz
In-house Transmitter node	-3.02	2.424
In-house Receiver node	-3.14	2.424
TI Evaluation nodes	-1.05	2.425

IV. DATA PROCESSING

A. Path Loss Analysis

Analytical and empirical propagation models have been well covered in the literature. Measurements, for both indoor and outdoor environments, have shown that the average received signal decreases logarithmically with distance. The mathematical approximation of power loss as a function of distance is defined by [45, 46]:

$$P_{rdBm} = P_{tdBm} - \left[PL(d_0)_{dB} + 10\gamma \log\left(\frac{d}{d_0}\right) + \chi_\sigma \right] \quad (1)$$

The term χ_σ in (1) represents distributed random variables modelled by a zero-mean Gaussian function, γ defines the path loss exponent and $PL(d_0)_{dB}$ is the initial path loss at reference distance (d_0), including antenna gains.

For the case of on/off-body communications, (1) not only includes antenna characteristics, but also human body shadowing (which depends on the user) and average channel attenuation, which is defined by the surrounding environment [15, 20]. A simplified path loss expression is defined by:

$$PL(d)_{dB} = PL(d_0)_{dB} + 10\gamma \log\left(\frac{d}{d_0}\right) \quad (2)$$

In our study, γ and $PL(d_0)_{dB}$ are derived from measured data considering a reference distance of 15 cm (d_0=15cm). Recorded data and least square (LS) fitting curves are shown in Fig. 7 for both VNA and sensor-based measurements.

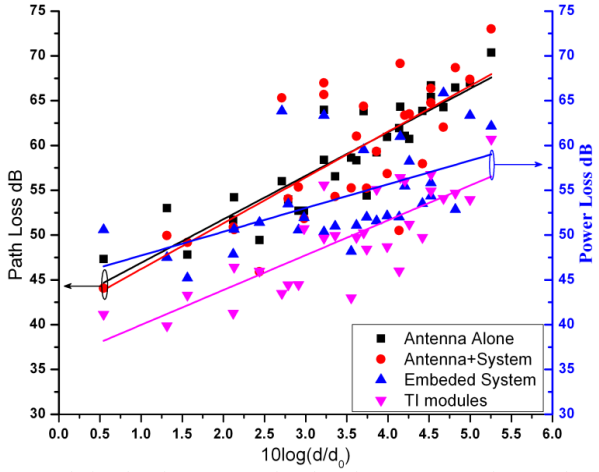

Fig. 7. Anechoic Chamber Measured Path and Power Loss values on the trunk section using LS linear fitting for: Stand Alone Antenna, Antenna with close proximity to the in-house wireless sensor, in-house wireless node with patch antenna and alternative wireless node using TI evaluation modules.

TABLE V
STATISTICAL PARAMETERS OF MEASURED ON-BODY PATH LOSS AT 2.42 GHZ FOR AN ANECHOIC ENVIRONMENT

Scenario	Median dB	Mean dB	PL(d_0) dB	γ	Root-MSE dB
Stand Alone Antenna (Fig. 4a)	58.93	58.84	42.03	4.86	2.74
Antenna with In-House System Behind (Fig. 4b)	58.65	58.77	41.09	5.11	5.06
In-House Embedded Wireless System (Fig. 5b)	52.09	54.23	45.06	2.65	4.63
Texas Instruments Evaluation modules (Fig. 5d)	49.74	49.54	36.08	3.89	3.27

The human body torso is formed by curvatures in both longitudinal and horizontal directions, which increase the shadowing effect in the wave propagation (Fig. 7); therefore, the use of flat, cylindrical or uniform dielectric phantoms can lead to inaccuracies in the estimation of path loss exponent.

Moreover, the use of directive antennas for on-body communications (microstrip patch antennas in our study) add to the spread of path-loss values around the linear fit (Fig. 7); therefore, the more directive the antenna is, the less linear is the relation between $PL(d)_{dB}$ and $\log(d/d_0)$. Important statistical parameters for each on-body setup are presented in Table V.

The results for all systems show high path-loss components, a product of high electromagnetic absorption along the human trunk and wave propagation alongside a non-uniform curvilinear surface. However, there is a noticeable difference between the results taken with the VNA and those made using the wireless sensor nodes, discussed below.

Although the projected path loss exponents differ between in-house wireless sensors and TI evaluation modules, 2.65 and 3.89 respectively, the values are comparable to the path loss exponents found by empirical, numerical and analytical methods reported in [47] (pair of microstrip patches), [23] and [48] (pair of dipoles), and [49] (pair of monopoles). Differences are attributed to the differences in size of the two systems (Fig. 5).

The in-house embedded nodes have a better performance with distance (γ=2.65), but have more radiation losses compared to the TI evaluation modules. However, measurements of the stand-alone on-body antennas prove to have higher losses than those integrated with on-body systems. This may be due to measurement uncertainties, such as cable effects (e.g., the presence of common mode currents or reflections from the VNA). It is noticeable that the presence of the system has a minimal effect when using the VNA technique, which may imply that the cable effect dominates.

The results in Fig. 7 show some discrepancies between those measured with the VNA and those using the wireless sensor modules, in terms of gradients (see also Table V). It is thought that this difference is partly due to the fact that the wireless nodes operate in a single channel with a maximum bandwidth of 5 MHz, whereas the VNA measurements were performed over the whole ISM bandwidth (80.5 MHz). Other factors include the cable effect and potential scattering from the wireless sensor node structure.

In order to further investigate possible causes of this effect, additional on-body measurements with the wireless nodes were performed at location 6 (being the largest distance on the human trunk, d=50.3 cm). The mean and standard deviation of the recorded sensor data, defined by (3) with N = 1 and N=2, respectively, are displayed in Fig. 8 and a summary is listed in Table VI.

$$\sigma_N = \sqrt{\frac{1}{N}\sum_{i=1}^{N}\left(x_i - \bar{x}\right)^2} \qquad (3)$$

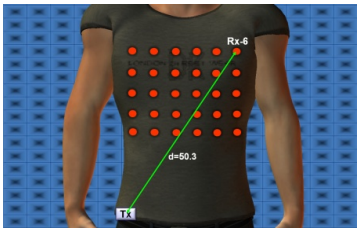

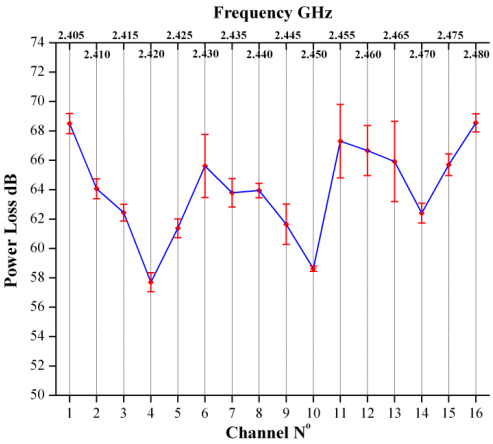

Fig. 8. Channel performance of receiving node located at the largest distance from the transmitter module: mean (line-plot) and standard deviation (error bars).

TABLE VI
MEAN AND STANDARD DEVIATION FOR EACH OF THE 16 CHANNELS IN THE 2.45 GHZ ISM BAND USING IN-HOUSE WIRELESS NODES FOR ON-BODY LOCATION 6

Channel N°	μ dB	σ dB	Channel N°	μ dB	σ dB
1	68.49	0.69	9	61.64	1.37
2	64.05	0.67	10	58.62	0.18
3	62.43	0.57	11	67.29	2.50
4	57.70	0.64	12	66.65	1.70
5	61.37	0.63	13	65.91	2.73
6	65.60	2.15	14	62.40	0.68
7	63.78	0.97	15	65.69	0.74
8	63.94	0.49	16	68.54	0.62

Most of the channels experience variations of 0.5 dB to 2 dB on the received signal. Channels *4* and *10*, operating at carrier frequencies of 2.42 GHz and 2.45 GHz, respectively, define the best communication links, with the smallest mean path loss values of 57.7 dB and 58.6 dB, respectively

(Table VI). Although the antennas have the best power transfer around 2.42 GHz (Fig. 2b), the performance of channel 10 is still good enough at 30 MHz away from the best radiation performance of the antennas.

On the other hand, channels 6, 11, and 13 exhibit average variations of 5 dB. For a wireless sensor programmed to operate at 2.43 GHz (i.e., channel 6), the variation in antenna radiation properties, such as the 10 MHz detuning observed at point 6 (Fig. 3), have produced a change in the antenna's return loss magnitude, which must contribute to the worse performance in these channels. It is further conjectured that, over a given time frame, the breathing process creates both LOS and NLOS propagation; thus, when the subject is stationary, shadowing is the dominant fading observed, especially when the largest distance along the trunk is considered (i.e., position 6). The communication link on channel *6* (f_c=2.43 GHz) is comparable to the mean path loss values of channels *1* and *16*, despite being only 10 MHz away from the antenna's operating frequency.

Fig. 9. Location of transmitter and receiver for on-body measurements using wireless sensor nodes at each carrier frequency.

TABLE VII
SUMMARY OF STATISTICAL PARAMETERS OF 16 DIFFERENT CHANNELS USING LOW POWER SENSORS

Channel N°	Frequency GHz	PL_{d0} dB	γ	Root-MSE dB
1	2.405	47.58	2.68	7.05
2	2.410	42.22	3.57	4.23
3	2.415	42.01	4.24	4.45
4	2.420	45.56	2.73	3.88
5	2.425	46.15	2.81	5.36
6	2.430	40.40	5.23	5.25
7	2.435	41.51	4.32	3.74
8	2.440	40.70	4.65	3.11
9	2.445	47.70	2.38	4.29
10	2.450	36.67	4.74	5.07
11	2.455	43.43	4.43	7.88
12	2.460	34.97	5.98	5.99
13	2.465	40.60	3.77	3.21
14	2.470	40.90	4.64	3.40
15	2.475	39.75	4.76	5.52
16	2.480	44.71	3.12	4.61

In order to have a better understanding of the carrier-frequency dependence, on-body measurements were extended further over 9 different points (Fig. 9) using the in-house wireless nodes. The recorded data was used to estimate path loss models for each carrier frequency. Measured values and least-square (LS) fitted path loss curves are shown in Figs. 10a and 10b. Fig. 10c shows the performance of each on-body radio channel and the main statistical parameters for each communication channel are described in Table VII.

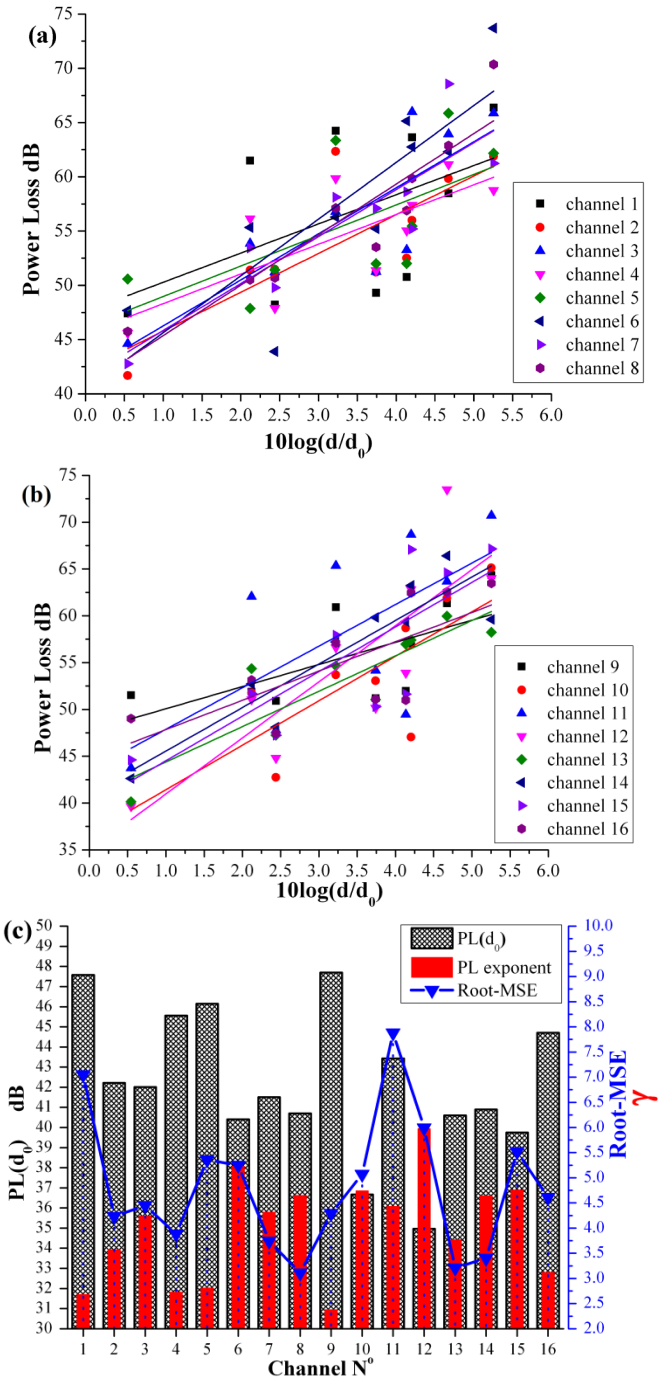

Fig. 10. Average Power Loss values using LS linear fitting for each frequency carrier at 2.45 GHz ISM band: (a) response of the first 8 channels; (b) response of the last 8 channels; (c) summary of statistical parameters of each frequency carrier.

If a static radio propagation analysis is followed, channel *4* provides the maximum and optimum power transfer and, hence, is the best carrier frequency. However, for on-body communications, even when the subject is motionless, channel performance changes dynamically due to small variations caused by internal human body processes. Results show that

channels *4* and *9* have the best communication links based on path loss exponents (γ_{CH-4}=2.73 and γ_{CH-9}=2.38, respectively); on the other hand, channels *6* and *12* have the highest path loss exponents (γ_{CH-6}=5.23 and γ_{CH-12}=5.98, respectively). If we consider the reference path loss, however, channel 9 exhibits the worst radio link (most loss) and 12 becomes the most suitable channel, in comparison to other adjacent channels.

It is evident that different channels have different characteristics; channel losses are a consequence not only of the presence of tissues with high permittivities, but also of the irregular surface of the torso. When the dynamic nature of the environment is considered, it is evident that optimum performance may require some degree of intelligence, in order to select the most appropriate channel (e.g., in terms of link reliability or minimising energy consumption).

In order to evaluate the performance of wireless sensors over the whole 2.45 GHz ISM band, the mean power loss was found for the sixteen carrier frequencies. Fig. 11 shows the LS linear fitting of this averaging, compared with the VNA-based measurements; Table VIII presents the statistical summary.

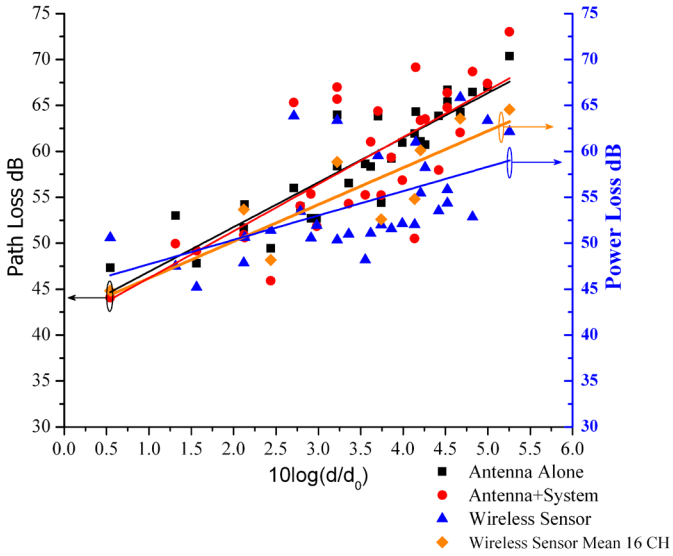

Fig. 11. Comparison of Average Path and Power Loss for: mean of all 16 channels using wireless sensors, initial VNA measurements and single frequency response.

TABLE VIII
SUMMARY OF STATISTICAL PARAMETERS FOR PATH AND POWER LOSS MEASURED BY: THE VNA (2.45 GHZ ISM BAND) AND IN-HOUSE WIRELESS NODES (SINGLE CHANNEL 2.42GHZ AND AVERAGE OF ALL 16 CHANNELS)

Scenario	Median dB	Mean dB	PL(d_0) dB	γ	Root-MSE dB
Stand Alone Antenna	58.93	58.84	42.03	4.86	2.74
Wireless Sensors (Single Channel)	52.09	54.23	45.06	2.65	4.63
Wireless Sensor (Mean 16-Channels)	54.83	55.69	42.18	4.00	3.4

B. *Cumulative Distribution Function*

In this analysis, the two different measurement techniques (i.e., using the VNA and using the wireless sensor modules) are compared on the basis of the cumulative distribution functions (CDF) as a function of average received power; these are shown in Fig. 12.

All parameters were calculated on a 95% confidence interval (CI), according to their maximum-likelihood (ML) estimates. The variation around the mean path loss is best described by a log-normal distribution (4) which is commonly used to model long-term fading (shadowing):

$$f(x|\mu,\sigma)=\frac{1}{x\sigma\sqrt{2\pi}}\exp\left\{-\frac{(\ln x-\mu)^2}{2\sigma^2}\right\} \quad (4)$$

The mean and variance of the log-normal random variable are denoted μ and σ^2, respectively, and are given in Table IX for each measurement setup. The data acquired by both VNA and wireless sensors shows compact behaviour in the first and third quartiles (i.e., below 52.15 dB and above 62.51 dB, respectively). However, the median quartile presents the most spread data.

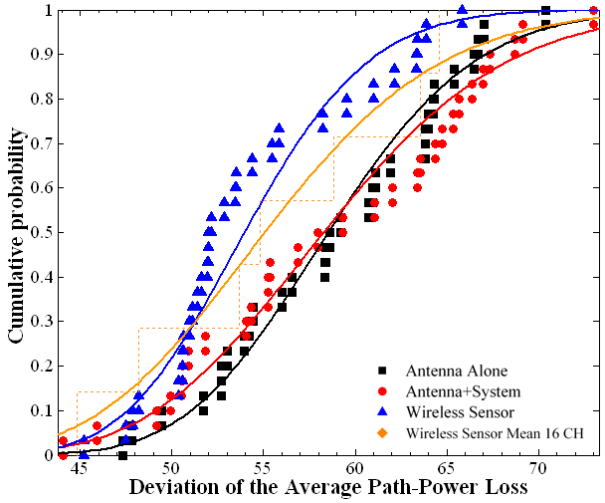

Fig. 12 Deviation of Measurements from the average Path and Power Loss

TABLE IX
AVERAGE VALUE AND STANDARD DEVIATION OF LOGNORMAL DISTRIBUTION APPLIED TO PATH AND POWER LOSS FOR MEASUREMENTS TAKEN WITH THE VNA (2.45 GHZ ISM BAND) AND IN-HOUSE WIRELESS NODES (SINGLE CHANNEL 2.42GHZ AND AVERAGE OF ALL 16 CHANNELS)

Scenario	Lognormal Fit	
	μ dB	σ dB
Stand Alone Antenna	4.06	0.106
Antenna with Sensor Behind	4.06	0.133
In-House Wireless Sensor (Single)	3.98	0.098
Wireless Sensor (Mean 16-Channels)	4.00	0.136

This trend is caused by two factors: first, the wireless sensor nodes are coupled to an embedded antenna, usually integrated with active and passive elements also assembled on the dielectric substrate; thus, the combination radiates as a whole structure. On the other hand, the stand-alone antennas do not have an adjacent structure that shields the wave propagation from the effects of the human tissue.

Second, the use of semi-rigid coaxial cables in the VNA measurements may introduce errors. For example, the excitation of surface currents on the outer metallic shield of coaxial cables (common mode currents) is unavoidable, causing pattern degradation. Furthermore, the presence of cables in the wave propagation path can scatter or even radiate electromagnetic waves, thus causing fragmentation, distortion of the antenna radiation pattern and signal variation from cable movements, even when not connected to the antenna. These may be exacerbated by the use of unbalanced antennas and designs with small ground planes.

V. Conclusions

On-body communication channels between two low-power IEEE 802.15.4 sensor nodes operating in the 2.45 GHz ISM band (2.40-2.4835 GHz) have been presented. Propagation measurements were performed on the trunk section of the human body in an anechoic environment, where multipath and scattering effects, usually present in an indoor environment, are negligible.

First, measurements were made using a standard VNA connected via coaxial cables. An alternative measurement technique for on-body antennas was then examined, utilising wireless sensors nodes. The latter not only diminished the effect of coaxial cables (scattering or radiation), but also provided a more realistic response of the radio link channel. The limitations of the VNA approach are evident when comparing the results shown in Figs. 7 and 11 (also Tables V and VIII), where the combination of cable effect and measurement bandwidth dominate over the physical proximity of a realistic system. The VNA measurements usually imply a path loss around 3 dB lower than that using the wireless sensor node approach, with equivalent differences in other measures. The path loss exponent is always found to be greater using the VNA method, often by a factor of 2. Hence, the value of the wireless sensor method can be seen in the more realistic data observed. Thus, the two techniques may be seen as complementary: the VNA approach has the benefits of greater speed and dynamic range, whilst the utilisation of sensor nodes allows a more detailed investigation of real-world scenarios.

The radio communication for each of the 16 IEEE 802.15.4 channels in the 2.45 GHz ISM band was measured at different points on the torso, using this technique. It was found that the wireless sensors operating at individual carrier frequencies have different responses; hence, system performance is influenced not only by the initial antenna response, but also by the channel selected. Moreover, mean path loss values for a motionless test subject are dependent on the curvature of the human torso, which is subject-specific (and, for instance, can vary considerably between fat and thin subjects); this impedes LOS signals (strong signals) and, hence, the path-loss characteristics exhibit dominant shadowing effects (weak signal).

Although the radiation of the antennas is normal to the body surface, measured data shows that physiological activities, such as the human breathing process and heart beat movements, affect the antennas' return loss, thus affecting communication throughput and system performance.

Furthermore, the miniaturization of wearable systems increases the fluctuations of individual radio links due to small and compact antenna designs. The new trend of wireless sensors with channel-sensing capabilities and radio performance algorithms are promising solutions; thus, channel and system performance can be optimized by dynamic scans between different channels linking different on-body nodes.

References

[1] P. S. Hall and Y. Hao, *Antennas and propagation for body-centric wireless communications*. Boston, Mass. ; London: Artech House, 2006.

[2] Y. Hao, R. Foster, *"Wireless body sensor networks for health-monitoring applications" (invited),* Physiol. Meas. 29, R27-R56, 2008.

[3] Z. H. Hu, M. Gallo, Q. Bai, Y. I. Nechayev, P. S. Hall, and M. Bozzettit, "Measurements and Simulations for On-Body Antenna Design and Propagation Studies," in *Antennas and Propagation, 2007. EuCAP 2007. The Second European Conference on*, 2007, pp. 1-7.

[4] M. Gallo, P. S. Hall, and M. Bozzetti, "Simulation And Measurement Of Body Dymamics For On-Body Channel Characteirisation," in *Antennas and Propagation for Body-Centric Wireless Communications, 2007 IET Seminar on*, 2007, pp. 71-74.

[5] M. Alexander, G. Palikaras, A. Sani, and M. Rajab, "Characterisation of low reflectivity antenna supports for electrically small antennas, and pattern measurement via optical fibre to eliminate common mode current errors," *Automated RF & Microwave Measurement Society (ARMMS),* 20-21 April 2009.

[6] L. Kin Seong, N. Mun Leng, and P. H. Cole, "Investigation of RF cable effect on RFID tag antenna impedance measurement," in *Antennas and Propagation Society International Symposium, 2007 IEEE*, 2007, pp. 573-576.

[7] P. J. Massey and K. R. Boyle, "Controlling the effects of feed cable in small antenna measurements," in *Antennas and Propagation, 2003. (ICAP 2003). Twelfth International Conference on (Conf. Publ. No. 491)*, 2003, pp. 561-564 vol.2.

[8] S. Saario, D. V. Thiel, J. W. Lu, and S. G. O'Keefe, "An assessment of cable radiation effects on mobile communications antenna measurements," in *Antennas and Propagation Society International Symposium, 1997. IEEE., 1997 Digest*, 1997, pp. 550-553 vol.1.

[9] P. A. Catherwood and W. G. Scanlon, "Measurement errors introduced by the use of co-axial cabling in the assessment of wearable antenna performance in off-body channels," in *Antennas and Propagation (EUCAP), Proceedings of the 5th European Conference on*, 2011, pp. 3787-3791.

[10] A. D. Olver, *Microwave and optical transmission*: Wiley, 1992.

[11] I. L. Chun and W. Kin-Lu, "Printed Monopole Slot Antenna for Internal Multiband Mobile Phone Antenna," *Antennas and Propagation, IEEE Transactions on,* vol. 55, pp. 3690-3697, 2007.

[12] L. Chung-Huan, E. Ofli, N. Chavannes, and N. Kuster, "SAR and efficiency performance of mobile phone antenna with different user hand positions," in *Antennas and Propagation Society International Symposium, 2009. APSURSI '09. IEEE*, 2009, pp. 1-4.

[13] A. Ikram, C. Beckman, and S. Irmscher, "Design and development of a multiband loop antenna for cellular mobile handsets," in *Antenna Technology (iWAT), 2011 International Workshop on*, 2011, pp. 251-254.

[14] P. S. Hall, M. Ricci, and T. M. Hee, "Measurements of on-body propagation characteristics," in *Antennas and Propagation Society International Symposium, 2002. IEEE*, 2002, pp. 310-313 vol.2.

[15] P. S. Hall, H. Yang, Y. I. Nechayev, A. Alomalny, C. C. Constantinou, C. Parini, M. R. Kamarudin, T. Z. Salim, D. T. M. Hee, R. Dubrovka, A. S. Owadally, S. Wei, A. Serra, P. Nepa, M. Gallo, and M. Bozzetti, "Antennas and Propagation for On-Body Communication Systems," *Antennas and Propagation Magazine, IEEE,* vol. 49, pp. 41-58, 2007.

[16] Z. H. Hu, Y. I. Nechayev, P. S. Hall, C. C. Constantinou, and H. Yang, "Measurements and Statistical Analysis of On-Body Channel Fading at 2.45 GHz," *Antennas and Wireless Propagation Letters, IEEE,* vol. 6, pp. 612-615, 2007.

[17] S. L. Cotton and W. G. Scanlon, "Statistical characterisation for a mobile bodyworn personal area network in an indoor multipath environment at 868 MHz," in *Antennas and Propagation, 2006. EuCAP 2006. First European Conference on*, 2006, pp. 1-7.

[18] S. L. Cotton and W. G. Scanlon, "Characterization and modeling of on-body spatial diversity within indoor environments at 868 MHz," *IEEE Transactions on Wireless Communications,* vol. 8, pp. 176-185, 2009.

[19] S. L. Cotton and W. G. Scanlon, "Characterization of the on-body channel in an outdoor environment at 2.45 GHz," in *Antennas and Propagation, 2009. EuCAP 2009. 3rd European Conference on*, 2009, pp. 722-725.

[20] S. L. Cotton and W. G. Scanlon, "An experimental investigation into the influence of user state and environment on fading characteristics in wireless body area networks at 2.45 GHz," *IEEE Transactions on Wireless Communications,* vol. 8, pp. 6-12, 2009.

[21] Z. Jian, D. B. Smith, L. W. Hanlen, D. Miniutti, D. Rodda, and B. Gilbert, "Stability of Narrowband Dynamic Body Area Channel," *IEEE Antennas and Wireless Propagation Letters,* vol. 8, pp. 53-56, 2009.

[22] E. Reusens, W. Joseph, B. Latre, B. Braem, G. Vermeeren, E. Tanghe, L. Martens, I. Moerman, and C. Blondia, "Characterization of On-Body Communication Channel and Energy Efficient Topology Design for Wireless Body Area Networks," *IEEE Transactions on Information Technology in Biomedicine,* vol. 13, pp. 933-945, 2009.

[23] E. Reusens, W. Joseph, G. Vermeeren, L. Martens, B. Latre, I. Moerman, B. Braem, and C. Blondia, "Path loss models for wireless communication channel along arm and torso: measurements and simulations," in *IEEE Antennas and Propagation Society International Symposium*, 2007, pp. 345-348.

[24] D. Smith, L. Hanlen, Z. Jian, D. Miniutti, D. Rodda, and B. Gilbert, "Characterization of the Dynamic Narrowband On-Body to Off-Body Area Channel," in *IEEE International Conference on Communications, 2009. ICC '09*, 2009, pp. 1-6.

[25] D. Smith, L. Hanlen, D. Miniutti, Z. Jian, D. Rodda, and B. Gilbert, "Statistical characterization of the dynamic narrowband body area channel," in *First International Symposium in Applied Sciences on Biomedical and Communication Technologies, ISABEL '08.* , 2008, pp. 1-5.

[26] D. B. Smith, Z. Jian, L. W. Hanlen, D. Miniutti, D. Rodda, and B. Gilbert, "A simulator for the dynamic on-body area propagation channel," in *IEEE Antennas and Propagation Society International Symposium, 2009. APSURSI '09*, 2009, pp. 1-4.

[27] D. B. Smith, J. Zhang, L. W. Hanlen, D. Miniutti, D. Rodda, and B. Gilbert, "Temporal correlation of dynamic on-body area radio channel," *Electronics Letters,* vol. 45, pp. 1212-1213, 2009.

[28] D. B. Smith, D. Miniutti, L. W. Hanlen, D. Rodda, and B. Gilbert, "Dynamic Narrowband Body Area Communications: Link-Margin Based Performance Analysis and Second-Order Temporal Statistics," in *IEEE Wireless Communications and Networking Conference (WCNC)*, 2010, pp. 1-6.

[29] Y. I. Nechayev, P. S. Hall, and Z. H. Hu, "Characterisation of narrowband communication channels on the human body at 2.45 GHz," *IET Microwaves, Antennas & Propagation,* vol. 4, pp. 722-732, 2010.

[30] Y. I. Nechayev, Z. H. Hu, and P. S. Hall, "Short-term and long-term fading of on-body transmission channels at 2.45 GHz," in *LAPC Antennas & Propagation Conference, Loughborough*, 2009, pp. 657-660.

[31] S. F. Heaney, W. G. Scanlon, E. Garcia-Palacios, and S. L. Cotton, "Fading characterization for Context Aware Body Area Networks (CABAN) in interactive smart environments," in *Loughborough Antennas and Propagation Conference (LAPC)*, 2010, pp. 501-504.

[32] V. G. Chaganti, D. B. Smith, and L. W. Hanlen, "Second-Order Statistics for Many-Link Body Area Networks," *IEEE Antennas and Wireless Propagation Letters,* vol. 9, pp. 322-325, 2010.

[33] A. Guraliuc, A. A. Serra, P. Nepa, G. Manara, F. Potorti, and P. Barsocchi, "Body posture/activity detection: Path loss characterization for 2.4GHz on-body wireless sensors," in *IEEE Antennas and Propagation Society International Symposium, APSURSI '09*, 2009, pp. 1-4.

[34] A. R. Guraliuc, A. A. Serra, P. Nepa, and G. Manara, "Channel model for on body communication along and around the human torso at 2.4GHz and 5.8GHz," in *International Workshop on Antenna Technology (iWAT 2010)*, 2010, pp. 1-4.

[35] L. W. Hanlen, D. Miniutti, D. Rodda, and B. Gilbert, "Interference in body area networks: Distance does not dominate," in *IEEE 20th International Symposium on Personal, Indoor and Mobile Radio Communications*, 2009, pp. 281-285.

[36] A. Zhang, L. W. Hanlen, D. Miniutti, D. Rodda, and B. Gilbert, "Interference in body area networks: Are signal-links and interference-links independent?," in *IEEE 20th International Symposium on Personal, Indoor and Mobile Radio Communications*, 2009, pp. 456-460.

[37] Texas Instruments. (2007). *2.4 GHz IEEE 802.15.4 / ZigBee-ready RF Transceiver*. Available: http://focus.ti.com/lit/ds/symlink/cc2420.pdf

[38] S. Gabriel, R. W. Lau, and C. Gabriel, "The dielectric properties of biological tissues: II. Measurements in the frequency range 10 Hz to 20 GHz," *Physics in Medicine and Biology,* vol. 41, pp. 2251-2269, 1996.

[39] Camilia Gabriel, "Compilation of the Dielectric Properties of Body Tissues at RF and Microwave Frequencies," Radiofrequency Radiation Division Brooks Air Force Base, Ed., ed. Texas, United States, 1996.

[40] Institute for Applied Physics - Italian National Research Council. (2007). *Calculation of the Dielectric Properties of Body Tissues*. Available: http://niremf.ifac.cnr.it/tissprop/htmlclie/htmlclie.htm#atsftag

[41] A. Alomainy, Y. Hao, A. Owadally, C. G. Parini, Y. Nechayev, C. C. Constantinou, and P. S. Hall, "Statistical Analysis and Performance Evaluation for On-Body Radio Propagation With Microstrip Patch Antennas," *IEEE Transactions on Antennas and Propagation,* vol. 55, pp. 245-248, 2007.

[42] Microchip. (2008). *PIC18F2620 28-Pin Enhanced Flash Microcontrollers with 10-Bit A/D and NanoWatt Technology*. Available: http://ww1.microchip.com/downloads/en/DeviceDoc/39626e.pdf

[43] IEEE 802.15.4 Standard. (2006). *Wireless Medium Access Control (MAC) and Physical Layer (PHY) Specifications for Low Rate Wireless Personal Area Networks (LR-WPANs)*. Available: http://standards.ieee.org/getieee802/download/802.15.4-2006.pdf

[44] C. A. Balanis, *Antenna theory : analysis and design*, 3rd ed. ed. Hoboken, N.J.: [Great Britain] : Wiley-Interscience, 2005.

[45] A. Goldsmith, *Wireless communications*. Cambridge: Cambridge University Press, 2005.

[46] T. S. Rappaport, *Wireless communications : principles and practice*, 2nd ed. ed. Upper Saddle River, N.J. ; [Great Britain]: Prentice Hall PTR, 2002.

[47] A. Sani, Z. Yan, H. Yang, A. Alomainy, and C. Parini, "An Efficient FDTD Algorithm Based on the Equivalence Principle for Analyzing Onbody Antenna Performance," *IEEE Transactions on Antennas and Propagation,* vol. 57, pp. 1006-1014, 2009.

[48] E. Reusens, W. Joseph, G. Vermeeren, and L. Martens, "On-Body Measurements and Characterization of Wireless Communication Channel for Arm and Torso of Human," in *4th International Workshop on Wearable and Implantable Body Sensor Networks (BSN 2007)*. vol. 13, S. Leonhardt, T. Falck, and P. Mähönen, Eds., ed: Springer Berlin Heidelberg, 2007, pp. 264-269.

[49] G. A. Conway, W. G. Scanlon, S. L. Cotton, and M. J. Bentum, "An analytical path-loss model for on-body radio propagation," in *International Symposium on Electromagnetic Theory (EMTS), URSI* 2010, pp. 332-335.

Max O. Munoz received the M.Eng. degree in Electronic Engineering from Queen Mary, University of London (QMUL), London, U.K., in 2008. He joined the Antennas and Electromagnetics Research Group at QMUL the same year and is currently pursuing the Ph.D. degree.

His current research interests include small and compact antennas for low-power wireless sensors, flexible body-worn antennas for medical applications, radio propagation characterization, indoor RF localization, modelling for body-centric networks, antenna interactions with the human body, design and development of low-power circuits, and RF instrumentation. He has published and presented papers in a number of established international conferences, including EuCAP and LAPC.

Robert Foster (M-08) received a first class M.Eng. degree in electronics and communications and the Ph.D. degree from the University of Birmingham, Birmingham, U.K., in 2004 and 2008, respectively.

Currently, he is the QUEST Research Programme Manager and Postdoctoral Researcher at Queen Mary College, University of London, London, U.K. He has authored or co-authored a number of conference and journal papers, including contributions in Proceedings of the IEEE and IEEE Transactions on Antennas and Propagation. His current research interests include body-centric wireless communications, wireless sensors, low-power systems, UWB systems, millimeter-wave systems, RF-based positioning systems, and RFID.

Dr. Foster is a member of the Institution of Engineering and Technology (IET), U.K. He is also a member of the IEEE Antennas and Propagation Society, the IEEE Microwave Theory and Techniques Society, the IEEE Communications Society and the IEEE Circuits and Systems Society. He has attended a number of established international conferences and presented invited talks at a number of events, including LAPC 2011 and the IET Seminar on Wireless Communication in Buildings, 2011. He has acted as a reviewer for a number of international journals, including Proceedings of the IEEE, IEEE Transactions on Antennas and Propagation and IEEE Antennas and Wireless Propagation Letters.

Yang Hao (M'00–SM'06) received the Ph.D. degree from the Centre for Communications Research (CCR) at the University of Bristol, Bristol, U.K., in 1998. He is currently a professor of antennas and electromagnetics in the Antenna Engineering Group, Queen Mary College, University of London. He is active in a number of areas, including computational electromagnetics, electromagnetic band-gap structures and microwave metamaterials, antennas and radio propagation for body centric wireless networks, active antennas for millimeter/sub-millimeter applications and photonic integrated antennas. He is a co-editor and co-author of the books Antennas and Radio Propagation for Body-Centric Wireless Communications (Boston, MA: Artech House, 2006), and FDTD modelling of Metamaterials: Theory and Applications (Boston, MA: Artech House, 2008), respectively.

Professor Hao is an Associate Editor for the IEEE Antennas and Wireless Propagation Letters, IEEE Transactions on Antennas and Propagation, International Journal of Antennas and Propagation and a honorary editor for the Chinese Journal of Radio Science. He was also a Co-Guest Editor for the IEEE TRANSACTIONS ON ANTENNAS AND PROPAGATION. He is a vice chairman of the Executive Team of IET Antennas and Propagation Professional Network and a member of the New Emerging Technology Committee of the IEEE Antenna and Propagation Society. He is also a member of Board of the European School of Antenna Excellence, a member of EU ASSIST Cost Action and the Virtual Institute for Artificial Electromagnetic Materials and Metamaterials, Metamorphose VI AISBL. He has served as an invited (ISAP07, LAPC07, IWAT08) and keynote speaker (ANTEM05, IWAT'10), a conference General Chair (LAPC08, Metamaterials09), a Session Chair and short course organizer at many international conferences. Professor Hao was elected as a Fellow of the ERA Foundation in 2007 and a Fellow of the IET in 2010.